

# ANALYSIS OF BATTERY CABLE FAULTS USING A DYNAMIC BATTERY MODEL

**Nosh K. Medora**  
**Managing Engineer, Electrical Practice**  
**Exponent Failure Analysis Associates, Inc.**  
**Phoenix, AZ 85027**

**Alexander Kusko**  
**Corporate Vice President, Electrical Practice**  
**Exponent Failure Analysis Associates, Inc.**  
**Natick, MA 01760**

## ABSTRACT

Fault current calculations for the selection of circuit breakers or fuses for battery cables is normally conducted for the voltage of fully charged batteries and cables at operating temperatures (Ref. 1). However, batteries at a low state of charge not only have a lower terminal voltage, but also have an internal resistance up to three times the nominal value (Ref. 2). Heating of the cables during a fault also increases the circuit resistance. The consequence can be a low fault current, with a time delay, or a failure of the fuses or circuit breakers to trip, possibly resulting in an ignition and fire. The problem is more acute when the voltage drop per unit length is high resulting in a power density per unit length that is high. Such a condition may occur in a nearly discharged battery in an electrically powered vehicle.

This technical paper uses a battery model generated from manufacturers' data sheet parameters to generate the appropriate terminal voltage and fault current as a function of the state of charge. This paper presents examples of battery fault current using the curves of Ref. 2. The paper will also address design and protection measures to avoid the hazard.

**Index Terms:** battery modeling, state of charge, fuse coordination, fault current, battery cable.

## INTRODUCTION

Rechargeable batteries are used as the source of electric power in several transportation applications, including hybrid and electric vehicles, electric wheelchairs, electric scooters, electric fork-lift trucks, and electric golf carts. Batteries are also used for backup systems such as in UPS (uninterruptible power systems) for computers, servers and data processing systems, and in telecommunication systems. In these systems, the modeling and simulation of power sources such as lead acid batteries is of utmost importance in predicting the normal operation of the system, and is also extremely important in predicting the electrical and mechanical parameters under fault conditions. An accurately modeled system will permit a reasonably accurate representation of the magnitude and duration of the fault current prior to the operation of the protective device such as a fuse or a circuit breaker. The fault current as a function of time is dependent on several parameters, including, but not limited to, fault resistance, geometrical dimensions of the cable, cable voltage drop, cable temperature rise, the state of charge (SOC) of the battery, prior number of cycles of operation of the battery, type of fuse, fuse time-current characteristics, operating current prior to fault, and ambient temperature.

This paper briefly summarizes the key selected battery parameters featured in the battery model of Ref. 2, and then uses these data sets in selected examples. Furthermore, this paper, will show that under certain conditions, when a battery is discharged to an SOC of less than 10 percent, such as during a deep discharge, and a fault occurs, the short-circuit current may not be of a sufficient magnitude to actuate the protection device in a reasonably short period of time, but yet may be high enough and be present for a period of time sufficient to cause significant damage and possibly an ignition of the cable insulation.

## DYNAMIC BATTERY MODEL

The dynamic battery model of Ref. 2 is a realistic engineering compromise between model complexity and accuracy and provides parameter flexibility with low simulation times. As presented in the Modeling Verification section of Ref. 2, the results demonstrate that this model provides a reasonable representation of the battery terminal voltage for the different discharge conditions. A further enhancement of this battery model is provided in Ref. 3 which includes a new enhanced model with increased accuracy; and also includes voltage, current, and power monitoring functions and further permits modeling of the cycle-by-cycle charge/discharge characteristics which is imperative for regenerative applications.

The battery model of Ref. 2 permits the user to incorporate manufacturers' electrical specifications and discharge curves of a typical off-the-shelf battery, and uses the data to generate the battery output characteristics for different operating profiles. Empirical equations and graphical representations were used to inter-relate various electrical variables including battery voltage, battery capacity, discharge current, internal resistance and battery SOC. Some of these equations and graphical representations will be used in this paper. Several key battery parameters are as follows (Ref. 2):

### **Battery Capacity**

Battery capacity in Amp-hour is defined as the stored charge that can be delivered to a constant current load, up to a pre-defined cut-off voltage. Battery capacity is dependent on several factors including, but not limited to the following: cell construction, shelf life, charge and discharge cycles, and temperature. The Amp-hour capacity of any group of cells may vary by  $\pm 20\%$  to  $\pm 50\%$  when shelf time, number of recharge cycles, manufacturing variances and possibly other factors are taken into account. (Ref. 2).

### **Battery Modeling**

The lead-acid battery was modeled using available data from the battery manufacturers' data sheets. This dynamic model uses manufacturers' data combined with algebraic equations which define the following (Ref. 2):

1. Battery capacity as a function of discharge current (Peukert's Equation).
2. Variable multipliers for adjusting model parameters at increasing discharge current.
3. Discharge voltage as a function of SOC.
4. Battery internal resistance as a function of SOC.

The selected battery was a sealed rechargeable lead-acid battery, Yuasa, DM55-12, 12V, 57-Ah and was modeled using the manufacturers' data sheet parameters and selected handbook curves.

### **DM55-12 - Selected Data Sheet Parameters (Ref. 4)**

- Nominal Voltage: 12 V.
- Nominal Capacity: 20 h rate of 2.85 A to 10.50 V, 57 Ah.
- Maximum discharge current with standard terminals 400 A.
- Maximum short duration discharge current: 600 A.
- Internal resistance of charged battery: 6 m $\Omega$  (approx.).

Fig. 1 presents the manufacturers' discharge curves for high discharge rate.

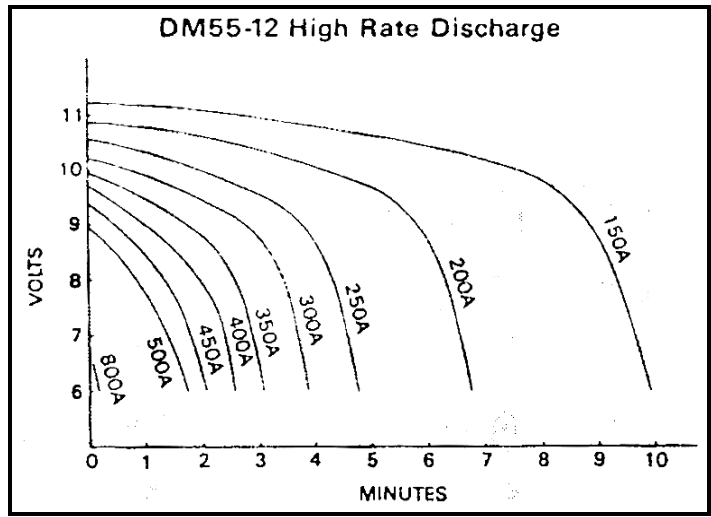


Fig. 1. Manufacturers' Discharge Curves for Yuasa, DM55-12, 12 V, 57 Ah High Discharge Rate (Ref. 4).

**Discharge Voltage as a Function of State of Charge**

The battery terminal voltage is a function of the state of charge of the battery. Fig. 2 presents the typical discharge profile and the algebraic equations showing the complex relationship between the cell voltage and SOC.

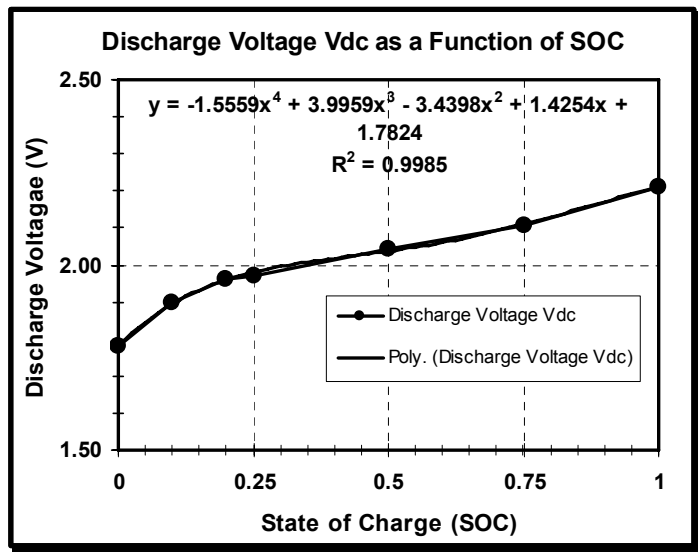


Fig. 2. Typical Discharge Profile for a Lead-Acid Battery (Ref. 2).

**Internal Resistance as a Function of State of Charge**

The battery internal resistance is a function of several variables, including aging of the cell, temperature and state of charge (Ref. 2).

## Aging

The internal resistance of the cell is fairly constant and only increases towards the end of life of the cell. The effects of aging have not been included in the model.

## Temperature

Temperature affects the resistive elements and the electrochemical elements in the cell. At high temperatures, the resistive elements increase in resistance. However, the resistivity of the electrolyte has a negative temperature coefficient and consequently its conductivity increases at higher temperatures. Temperature effects have not been incorporated in the model.

## State of Charge (SOC)

When the cell is fully charged, the internal resistance is at its nominal value. As the cell discharges, the internal resistance increases gradually. At approximately 25% SOC, the internal resistance increases rapidly. The battery model in this paper uses the curve of Ref. 2 to model the change in internal resistance as a function of the SOC of the battery. Fig 3 presents the change in internal resistance as a function of SOC of a typical lead-acid battery. It is observed that the internal resistance of the battery increases by a factor of approximately 3 as the SOC varies from 100% to 2.5%.

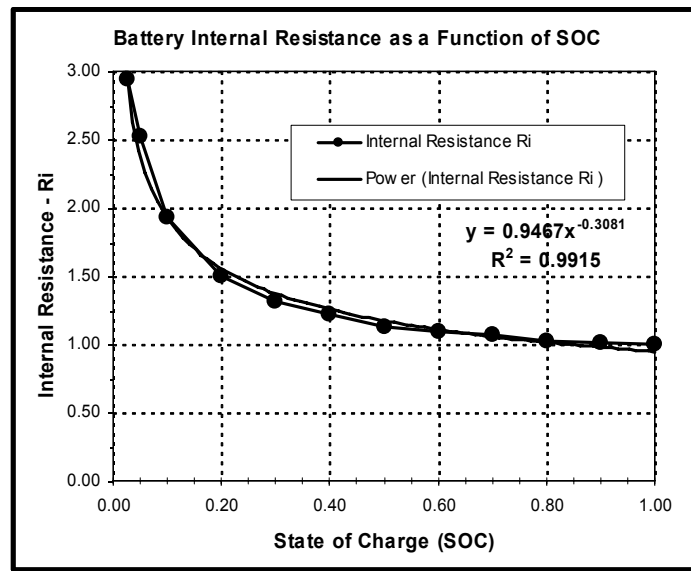


**Fig. 3. Internal Resistance Multiplier as a Function of State of Charge of a typical Lead-Acid Battery (Ref. 2).**

## BATTERY CABLES

A battery bank can contribute a substantial and sustained current into a short circuit in the battery cables or the supplied load. The battery bank and cables are protected from damage due to fault currents by a variety of devices such as current limiters, dc fuses or dc circuit breakers. The current rating of the protection device is typically based on the ampere rating of the battery cables, and is defined by a standard for example, the National Electrical Code (NEC).

The length of the battery cables varies with the application. Battery cables may be of a short length, for example, less than six feet, in applications involving transportation systems. On the other hand, battery cables may be relatively long, for example, over fifty feet, in applications like UPS where the batteries must be located where their weight can be tolerated. In systems involving UPS, because of the high value of each volt of battery voltage, the cables are typically sized taking into consideration several factors including the cable voltage drop.

## VERIFICATION OF REDUCED BATTERY CURRENT FOR SOC LESS THAN 10%

As mentioned earlier, when a battery is discharged to an SOC of less than 10 percent, such as during a deep discharge, and a fault occurs, the short-circuit current will be reduced in magnitude. This section presents verification of this concept using test data.

### Variables Used

1. An SC-60 fuse rated at 60 A is used to illustrate the concept. The fuse characteristics are included as Ref. 5.
2. The battery voltage is obtained from measured data. For two 12-Vdc batteries, and SOC ~ 90%,  $V_{batt} \sim 25.8$  Vdc and for SOC ~ 10%,  $V_{batt} \sim 22.5$  Vdc).
3. Battery type MK2. Battery capacity = 50.6 Ah at 20-hr rate. Battery internal resistance ~ 9 mΩ. The battery internal resistance multiplier is obtained from Fig. 3. The above electrical system consists of two batteries in series. For 100% SOC,  $R_{i0} = 9$  mΩ; at 10% SOC,  $R_{i1} = 1.92 \times 9$  mΩ = 17.3 mΩ.

The results of the fault current calculation are presented in Table 1. Figs. 4-5 present the voltage and current waveforms.

**Table 1 - Comparison of Parameters of the Fault Current Calculations for Battery SOC approximately 90% and 10%.**

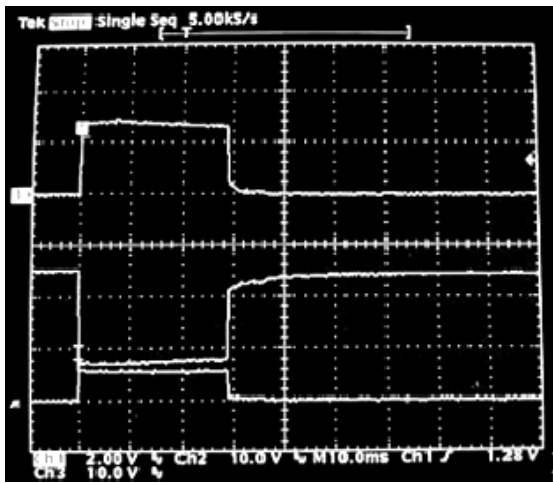
No.	Parameter	Battery SOC ~ 90%	Battery SOC ~ 10%
1.	Fuse Type	Bussmann SC-60	Bussmann SC-60
2.	Fuse Rating	60 A	60 A
3.	Battery Internal Resistance Multiplier	~ 1.00	~ 1.92
4.	Internal resistance of two batteries in series	~ 18 mΩ	~ 34.6 mΩ
5.	Fuse Clearing Time (measured)	~ 32 ms	~ 410 ms
6.	Fault Current at instance of fault (measured)	~ 675 A	~ 375 A
7.	Fault Current at instance of fault (calculated)	-	~ 411 A
8.	Percent difference in measured and calculated fault current	-	9.6%

### Summary

Thus, for the battery at 10% SOC, the calculated short circuit current of 411 A agrees well with the measured short circuit current of 375 A. The difference in the measured and calculated short circuit currents is less than 10%. This verifies the concept and the data curves.

For an almost fully charged battery, SOC ~ 90%, short circuit current  $I_{sc} \sim 675$  A, and 60-A, SC-60 fuse opens in ~ 32 ms.

For an almost discharged battery at ~ 10% SOC, short circuit current at instant of fault  $I_{sc} \sim 375$  A and the 60-A, SC-60 fuse opens in ~ 410 ms.

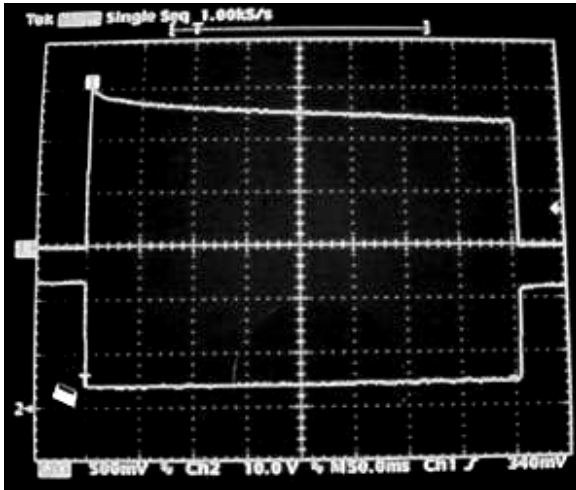


Short Circuit Current  $I_{sc} \sim 675$  A  
 60-A SC-60 Fuse opens in  $\sim 32$  ms

Top Waveform: Fault Current: 500 A/div.

Middle Waveform: Battery Voltage: 10V/div.  
 Bottom Waveform: Voltage downstream of Fuse: 10 V/div.  
 Time: 10 ms/div.

**Fig. 4. Voltage and Current Waveforms for an Almost Fully Charged Battery, SOC  $\sim 90\%$ .**



Short Circuit Current at Instant of Fault  $I_{sc} \sim 375$  A  
 60-A SC-60 Fuse opens in  $\sim 410$  ms

Top Waveform: Fault Current: 125 A/div.

Bottom Waveform: Battery Voltage: 10V/div.  
 Time: 50 ms/div.

**Fig. 5. Voltage and Current Waveforms for an Almost Discharged Battery, SOC  $\sim 10\%$ .**

**FAULT CURRENT CALCULATION – HIGH POWER DENSITY**

A fault current calculation is presented here which was performed for a battery powered dc circuit with the cable size selected based on its ampacity. The objective of this calculation was to demonstrate that with an almost discharged battery, and under certain system conditions, the fault current may reduce to a low value, resulting in a longer fuse opening time, with the result that there may be an increased temperature rise in the cable with the potential to thermally damage the cable insulation. Under extreme conditions, the high temperature rise in the cable may result in an ignition of the cable insulation. The power density per unit length is calculated and, in a succeeding section will be compared to the power density for cables used in a typical UPS. As shown in this section, the power density is relatively high for this test condition.

**Variables Used**

- Battery: Four 12-V batteries in series, for example Yuasa DM55-12, 12 V, 57 Ah.
- Internal Resistance of fully charged battery = 6 mΩ.
- Cable: Loop L = 5 ft, No. 10 AWG copper wire.
- Fuse: TRS-RDC Time Delay, DC rated 100 A (Ref. 6).

Calculation of short-circuit current and the fuse clearing time for battery SOC = 100% and SOC = 10%.

- Battery voltage: The battery discharge voltage is shown in Fig. 2 as a function of SOC (Ref. 2). For SOC = 100%,  $V_{batt} \sim 53.0$  Vdc. For SOC = 10%,  $V_{batt} \sim 45.0$  Vdc.
- Battery resistance: The internal resistance per battery as a function of SOC is show in Fig. 2 (Ref. 2). The internal resistance at SOC = 100% and for four batteries is  $R_{i0} \sim 4 \times 6 \times E-3 \sim 24$  m $\Omega$ . For SOC = 10%, the internal resistance is  $R_{i0} \sim 1.92 \times 24 \sim 46.1$  m $\Omega$ .
- Cable resistance:  $R_c = 5 \times 1.0$  m $\Omega$ /ft = 5 m $\Omega$ . Weight of copper = 71.3 g. Connector contact resistances  $R_{ct} \sim 2$  m $\Omega$ .
- Cable voltage drop per meter length =  $(40 \times 0.001 \times 3.281) = 0.131$  V
- Cable arcing fault: assume  $V_{arc} = 13$  V.
- The fuse time-current characteristics are presented as Ref. 6.
- Specific heat of copper = 385 J/kg . K

The fault current for the battery SOC ~ 100% is calculated, and the fuse clearing time is determined from the fuse characteristics. The fault current for battery SOC ~ 10% is also calculated using an iterative process, since it is decreasing, due to several factors including, but not limited to increase of cable resistance with increasing temperature and reduction in battery voltage as a function of time.

Table 2 presents a comparison of several parameters for battery SOC ~ 100% and battery SOC ~ 10%.

**Table 2 – Fault Current Calculation – High Power Density in Cable for Battery SOC approximately 100% and 10%.**

No.	Parameter	Battery SOC ~ 100%	Battery SOC ~ 10%
1.	Conductor Size	10 AWG	10 AWG
2.	Conductor Rating per NEC 2005, Table 310.16	40 A, 90 °C, TBS	40 A, 90 °C, TBS
3.	Nominal Load Current	40 A	40 A
4.	Fuse Rating and Type	TRS-RDC 100 A	TRS-RDC 100 A
5.	Fault Current	~ 1300 A	~ 500 A
6.	Current Density, in Cable per NEC 2005, Table 310.16	7.60 A / mm <sup>2</sup>	7.60 A / mm <sup>2</sup>
7.	Power Density/m/ x-section area	1.00 W /m /mm <sup>2</sup>	1.00 W /m /mm <sup>2</sup>
8.	Nominal Voltage Drop per m	131 mV/m	131 mV/m
9.	Fuse Clearing Time	~ 0.15 s	~ 13 s
10.	Cable Temperature	Minimal rise in temperature	~ 1040 °C

This high temperature is further verified by the Fusing Current Time Curves for copper wire listed in Ref. 7 and presented as Fig. 6. These fusing current curves show that a 10 AWG copper conductor carrying 500 A will fuse in ~ 8 s, and consequently will reach the melting temperature of copper which is approximately 1083 °C, assuming that "... radiation may be neglected owing to the short time involved, that is, 10 s ..." (Ref. 7).

Calculations indicate that in this system, the ratio of the voltage drop (IR) to the cross-section area is relatively high, and thus the power density per unit length is high. Thus, when a cable is selected such that the power density per unit length is high, then during a fault condition, with low SOC on the battery, the cable temperature rise may be relatively high.

It is therefore important in ampacity based cables, where the power density is relatively high, that not only does the cable have to be adequately sized for normal operation and fault protection included, but an additional measure of safety should also be provided, perhaps by using an under-voltage protection circuit, to disconnect the battery when the SOC decreases below a pre-determined level.

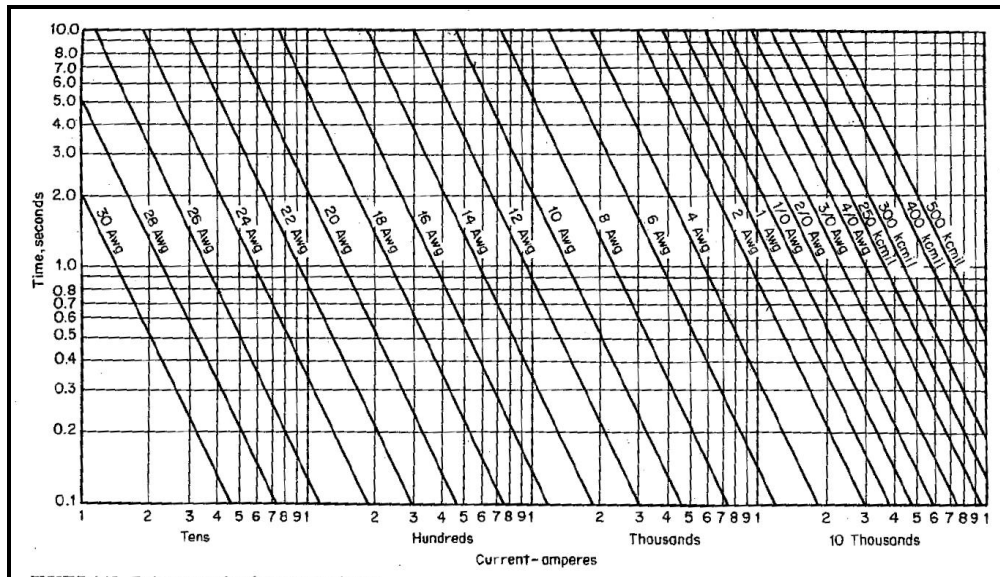


**Fig. 6. Fusing Current Time for Copper Conductors (Ref. 7).**

**FAULT CURRENT CALCULATION – UPS BATTERY CABLE - LOW POWER DENSITY**

A calculation was performed in the previous section, to determine the temperature rise during a fault in a system with an almost discharged battery connected to a cable with its size based on its ampacity, with the power density being relatively high. In this case, it was determined that the fault current may be low enough resulting in a relatively long time before the fuse clears, allowing the cable insulation to overheat prior to the fuse clearing.

Similar fault current calculations were also conducted for a battery powered circuit using a long cable, with the cable size selected based on its voltage drop. Typically, in UPS, because of the high value of each volt of battery voltage, the cables are sized taking into consideration several factors including cable voltage drop. IEEE Std 1184-2006, “IEEE Guide for Batteries for Uninterruptible Power Supply Systems” (Ref. 8), states, “... Cable voltage drop due to undersized cable can be a major factor in shorter than expected run times (see 7.5.2 for an example of sizing).” Ref. 8, Section 7.5.2 gives an example where the cable voltage drop is 2.1 V (~ 0.5%) in a UPS with a 405 to 430 V normal float voltage range.

Calculations summarized here, indicate that this low voltage drop, results in minimum power density in the cable, and consequently the cable typically has a small temperature rise, even under fault conditions. Thus, in a dc application, where a cable is selected using the voltage drop criteria, with low power density, not only does the load get the full voltage of the battery, but there is an additional benefit in that even under low SOC on the battery, the cable temperature rise is minimal.

**Calculations**

Ref. 8 presents a sample application of a three-phase UPS with cable sized by voltage drop. Calculations similar to those in the previous section were performed to determine the temperature rise in the cables for a fault occurring with an almost discharged battery. Selected information of this sample application obtained from Sec 7.5 of Ref. 8 is presented here:

### 7.5 Sample application: three-phase UPS

System size: 500 kva at 0.80 power factor = 400 kW [see Equation (2)]  
 System ac output voltage: 3 phase, 120/208 V (not required for calculation)  
 Inverter efficiency: 0.92 efficiency at full load (dc input to ac output)

...

Per NEC [B11] Table 310.16, a 750 kcmil (380 mm<sup>2</sup>) conductor is rated for up to 475 A × 4 conductors = 1900 A

...

Calculating for 100 m of cable =  $0.0563 \times 100/1000 = 0.00563$  ohms

Use Ohm's Law to calculate voltage drop

$$E = IR$$

$$E = 1500/4 \times .00563 = 2.1 \text{ V}$$

The battery terminal voltage then needs to be 2.1 V greater than the minimum load voltage. A minimum calculated battery voltage of 292 V is practical.

Table 3 presents a comparison of several parameters for high power density and low power density cables for battery SOC ~ 10%. Calculations indicate that for the low power density cable, due to the low cable voltage drop compared to the cross-section area, the power density per unit length is low and consequently even under fault conditions, the temperature rise is minimal. In this case, it is observed that the power density of 0.021 W /m /mm<sup>2</sup> is only ~ 2% of the power density of 1.00 W/m/mm<sup>2</sup> obtained in the previous section. Thus, when a cable is selected such that the ratio of the voltage drop to the cross-section area is relatively low, the power density is low and during a fault, even with a low battery SOC, the cable temperature rise is minimal.

**Table 3 – Comparison of Parameters - High Power Density and Low Power Density Cables, Battery SOC ~ 10%**

No.	Parameter	High Power Density Cable	Low Power Density Cable
1.	Conductor Size	10 AWG	4 x 750 kcmil
2.	Conductor Rating per NEC 2005, Table 310.16	40 A, 90 °C, TBS	535 A, 90 °C, TBS
3.	Nominal Load Current	40 A	1500 A
5.	Fault Current	~ 500 A	~ 13.0 kA
6.	Current Density in Cable per NEC 2005, Table 310.16	7.60 A / mm <sup>2</sup>	1.41 A / mm <sup>2</sup>
7.	Power Density/m/ x-section area	1.00 W /m /mm <sup>2</sup>	0.021 W /m /mm <sup>2</sup>
8.	Nominal Voltage Drop per m	131 mV/m	21 mV/m
9.	Fuse Clearing Time	~ 13 s	~ 5 s
10.	Cable rise in temperature under fault conditions	~ 1040 °C	Minimal rise in temperature

## CONCLUSIONS

1. During the protection and co-ordination study, the internal resistance of the battery as a function of SOC must be taken into account when coordinating battery cable size with the time-current characteristics of the protective device.
2. The curves of Fig. 2 and Fig. 3 can serve as a guide in the design of battery cables and protection systems.
3. For ampacity based cables, where the power density is relatively high, the cable voltage drop per meter length is relatively high. For voltage drop based cables, where the power density is relatively low, the cable voltage drop per meter length is low.
4. When a cable is selected such that the ratio of the voltage drop to the cross-section area is relatively high, the power density will probably be high, and consequently under fault conditions, with a low SOC on the battery, the cable temperature rise may be excessively high.
5. When a cable is selected such that the ratio of the voltage drop to the cross-section area is relatively low, the power density will probably be low, and consequently even under fault conditions, with a low SOC on the battery, the cable temperature rise is minimal.
6. For ampacity based cables, where the power density is relatively high, it is important that the cable be adequately sized for normal operation. The fuse must be selected to provide appropriate protection under all conditions including low battery SOC. It may be prudent to also provide an additional measure of safety perhaps by using an under-voltage protection circuit, to monitor and possibly disconnect the battery when the SOC decreases below a pre-determined level.
7. When a cable is selected such that the voltage drop per unit length is low, the power density will probably be low and consequently not only will the load get almost the full voltage of the battery, but there is an additional benefit in that even under fault conditions, with a low SOC on the battery, the cable temperature rise is minimal.

## REFERENCES

1. Tanaka, T, Yamasaki, M, “*Modeling of Fuses for Melting Time and Fusing Current Analysis*,” INTELEC 2004, pps. 671-675.
2. Medora, N. K., Kusko, A, “*Dynamic Battery Modeling of Lead-Acid Batteries Using Manufactures’ Data*”, Publication in the 27th International Telecommunications Energy Conference (INTELEC 2005), Proceedings, September 18-22, 2005, Berlin, Germany, pps. 225-230.
3. Medora, N. K., Kusko, A, “*An Enhanced Dynamic Battery Model of Lead-Acid Batteries Using Manufactures’ Data*,” Presentation, 28th Annual International Telecommunications Energy Conference (IEEE INTELEC 2006), Rhode Island Convention Center, Providence, RI, September 10–14, 2006. Also approved for publication in the IEEE INTELEC 2006 Conference Proceedings, pps. 293-300.
4. Data Sheet - Yuasa, DM55-12, 12 V, 57-Ah, Yuasa, Reading, PA, Rev 8/00.
5. Data Sheet - Fuse Characteristics, Bussmann SC-60 Time-Delay Fuse.
6. Data Sheet - Fuse Characteristics, Ferraz Shawmut TRS-RDC Time Delay / DC Rated Fuse, current rating 100 A.
7. Fink, D, Beaty, H., “*Standard Handbook for Electrical Engineers*”, Fourteenth Ed., © 2000 McGraw-Hill Companies, pps. 4-81-4-82.
8. IEEE Std 1184-2006, “IEEE Guide for Batteries for Uninterruptible Power Supply Systems” pps. 11-22.